PAPER • **OPEN ACCESS**

Fracture toughness to assess the effect of trimming on the fatigue behaviour of high-strength steels for chassis parts

To cite this article: S Parareda *et al* 2023 *IOP Conf. Ser.: Mater. Sci. Eng.* **1284** 012073

IOP Conf. Series: Materials Science and Engineering 1284 (2023) 012073 doi:10.1088/1757-899X/1284/1/012073

Fracture toughness to assess the effect of trimming on the fatigue behaviour of high-strength steels for chassis parts

S Parareda[1], D Frómeta[1], D Casellas[1,2], D Gustafsson[2], E Olsson[2], R Munier[3], A Mateo[4]

[1] Eurecat, Centre Tecnològic de Catalunya, Unit of Metallic and Ceramic Materials, 08243 Manresa, Spain
[2] Division of Solid Mechanics, Luleå University of Technology, 971 87 Luleå, Sweden
[3] ArcelorMittal Maizières Research & Development, BP 30320, F-57283 Maizières-les-Metz Cedex, France
[4] CIEFMA – Department of Materials Science and Engineering, EEBE, Universitat Politècnica de Catalunya-BarcelonaTech, 08019 Barcelona, Spain

Email: sergi.parareda@eurecat.org

Abstract. High-strength steels are widely used in vehicle body-in-white, offering a good balance between crashworthiness and lightweight design. The increased requirements of heavier electric vehicles, in terms of fatigue resistance and crashworthiness, highlight that chassis parts have remarkable lightweighting potential. However, applying these grades in chassis parts is not straightforward, as the forming processes, like trimming, may introduce surface defects that compromise the fatigue resistance of the component. This work presents a material selection strategy for the applicability of high-strength steels in chassis parts of electric vehicles. The proposed approach allows the evaluation of the key parameters of the chassis parts in a simple way. The crash performance is evaluated through fracture toughness using the essential work of fracture (EWF) methodology. The method is applied to thin high-strength steel sheets employing double-edge notched tensile specimens (DENT). On the other hand, fatigue performance is investigated in terms of fatigue resistance for both notched and unnotched specimens. The results for different complex-phase and dual-phase steels show a good agreement between the EWF and the fatigue notch factor. The method could help apply high-strength steel to chassis parts, as designers will have a tool to focus the expensive fatigue tests on the best material candidates.

1. Introduction

Using high-strength steels in car body-in-white (BiW) is a well-established strategy for lightweighting. Although the utilization of these materials has been focused on the BiW, they can also be used in chassis parts, which represent over 20% of the structural weight of the car. This approach becomes more and more relevant in the battery electric vehicles, as the heavy batteries increase their structural requirements. Besides the required exceptional crashworthiness behaviour, the chassis parts must deal with cyclic loads that can compromise the structural integrity of the vehicle. An improved fatigue resistance will help to reduce the weight of the vehicle by gauge reduction, which also contributes to the use of less material. This goal should be easily achieved by using high-strength steels with a yield strength close to (or even above) 1000 MPa, as it is well-accepted that an increasing linear trend exists between yield strength and fatigue resistance. However, when a defect is present in the material, this linear relationship is not valid anymore, and an increase in fatigue resistance is harder to obtain.

Fatigue resistance is a local plastic deformation occurring at high stressed points of the material, either in an intrinsic defect, as an inclusion or discontinuity in the microstructure, or an extrinsic defect, as a notch in the surface. When dealing with chassis parts, the extrinsic defects are related to the manufacturing operations like trimming or punching. It has been shown that the edge morphology depends on the material, shearing clearance and punch geometry, including the wear of the tool [1]. The edge geometry becomes crucial when dealing with local formability, as a lousy edge quality could lead to edge-cracking issues. These barriers were addressed through new approaches, such as fracture toughness to understand better the fracture behaviour of new materials and propose solutions to avoid fracture issues during part forming or develop materials with high cracking resistance. Previous works showed that tougher materials are more tolerant to the edge damage induced in sharing [2]. Additionally, improving the edge quality is beneficial for local formability, as shown in the hole expansion tests [3]. Similarly, improving the edge geometries by reducing the fracture zone or the burr is proven to be effective in enhancing fatigue resistance. A clear example is the utilization of the double-shearing strategy [4]. In this case, the consecutive shearing process removes a thin layer of damaged material, leaving a smoother edge with less damage than after the first cutting operation. Post-forming operations, like sandblasting or shot peening, also improve surface quality by smoothing the edge surface, rounding the edge corners, and introducing compressive residual stresses [5]. The coining processes that plastically deform the edge surface can also introduce these beneficial residual stresses. Although the mentioned operations can improve fatigue resistance, fatigue strength is still reduced because of the shearing process, which becomes critical in materials with high tensile strength.

Many factors affect the fatigue resistance of sheared edges, so developing solutions to improve the fatigue behaviour is time-consuming. Accordingly, some works addressed the development of rapid testing methodologies to shorten the testing time. Regarding the mechanical behaviour of sheared edges, the use of the material property that informs about damage tolerance, i.e. the fracture toughness, could bring valuable information to understand their fatigue resistance. Thus, this work proposes to combine the rapid testing of the fatigue limit in smooth specimens with fracture toughness values to estimate the fatigue notch factor of high-strength steels. The correlation between these properties could become a powerful material selection tool for fatigue applications of chassis parts with sheared or trimmed edges.

2. Materials and experimental procedure

The three materials studied in this work belong to the Advanced High Strength Steels (AHSS) family. The materials supplied by ArcelorMittal are two Complex Phase (CP) and a Dual Phase (DP) steel. HR CP800 SF is a hot rolled (HR) steel with a microstructure composed of bainitic-ferritic matrix with martensite and austenite islands, specially designed for a very good Stretch Flangeability (SF). Higher tensile strength is achieved by the HR CP980 SF thanks to the complex microstructure composed of tempered martensite and ferrite, combined with upper bainite and retained austenite islands, as shown in figure 1. Both CP steels exhibit good formability, while the HR DP600 steel perfectly balances formability and strength by combining a soft ferrite matrix with martensite islands. This combination leads to an outstanding strain hardening and elongation at fracture. The rough chemical composition of the investigated materials is given in table 1.

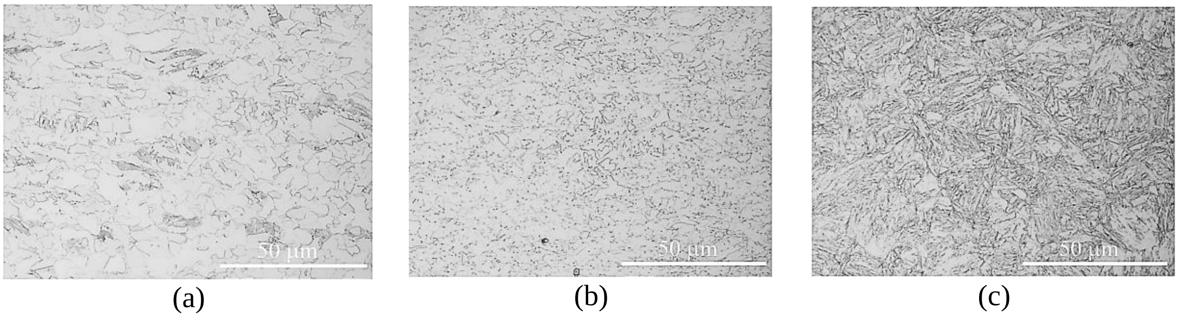

(a) (b) (c)

Figure 1. Microstructure of: a) HR DP600, b) HR CP800 SF, and c) HR CP980 SF.

Table 1. Chemical composition of the investigated materials in weight percentage. Balance is Fe.

Steel grade	C	Si	Mn	Cr	Al
HR DP600	≤ 0.10	≤ 0.30	≤ 1.50	≤ 0.90	≤ 0.06
HR CP800 SF	≤ 0.18	≤ 1.00	≤ 2.20	≤ 1.00	0.015-1.2
HR CP980 SF	≤ 0.20	≤ 1.00	≤ 2.20	≤ 1.00	0.015-1.2

Conventional tensile tests were carried out in an universal testing machine equipped with an extensometer and according to ISO6892-1 standard. The tensile specimens were machined at 90º concerning the rolling direction (RD). The specimen type 2 geometry from ISO 6892 with an L_0 of 80 mm was used. The tensile results are summarized in table 2.

Table 2. Mechanical properties in terms of yield strength (σ_{YS}), ultimate tensile strength (σ_{UTS}) and elongation at fracture (A_{80}, gauge length 80 mm).

Steel grade	t [mm]	σ_{YS} [MPa]	σ_{UTS} [MPa]	A_{80} [%]
HR DP600	4.3	439	622	21
HR CP800 SF	3.4	778	835	17
HR CP980 SF	3.5	957	1034	13

2.1. Fatigue tests

Fatigue behaviour was evaluated using hourglass specimens following the ISO 1099 standard. Specimens with a radius of 100 mm were machined by spark erosion at 90º concerning the RD and edge polished to a specular finish or trimmed. The gap between the punching and the die in the trimming tool was 0.3 mm, which means a trimming clearance of 7% for the DP600, 8.8% for the HR CP800 SF and 8.6% for the HRCP980 SF. This range of clearances is commonly used in the chassis parts. A drawing of the specimen geometry is shown in figure 2. The fatigue limit (σ_f) was defined at 10^6 cycles, $2{\cdot}10^6$ cycles. It was evaluated using the staircase or up-and-down method proposed by Dixon-Mood [6] and the *stiffness method* for the polished and trimmed conditions. At least 15 specimens were tested at room temperature for the conventional fatigue test, using a stress ratio of R = 0.1 and a frequency of 30 Hz. The obtained fatigue limit will be compared with results obtained by the rapid testing approach to check its accuracy.

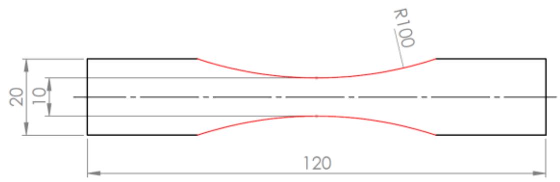

Figure 2. Hourglass fatigue specimen (K_t = 1.03) with the polished edge (in red colour). Dimensions are expressed in mm.

The *stiffness method* relies on the measurement of the fatigue damage through the determination of the specimen inelastic strains ($\Delta\varepsilon_p$) after each successive fatigue block [7]. The $\Delta\varepsilon_p$ is then plotted against the maximum stress (σ_{max}) of each block. The σ_f was determined as the interception of the fitting line to the x-axis, as schematically shown in figure 3. The length of the fatigue blocks was 6000 cycles, with increasing stress of 25 MPa between each one. For the $\Delta\varepsilon_p$ determination, the stress was set at $\sigma_{YS}/2$. At least three specimens were tested for each material and condition, all at room temperature and using a stress ratio of R = 0.1. Tests were performed in a servo-hydraulic testing machine MTS 322 Test Frame, at a frequency of 30 Hz, equipped with a Digital Image Correlation (DIC) system GOM Aramis SRX for $\Delta\varepsilon_p$ measurements using a virtual extensometer with a length of 40 mm.

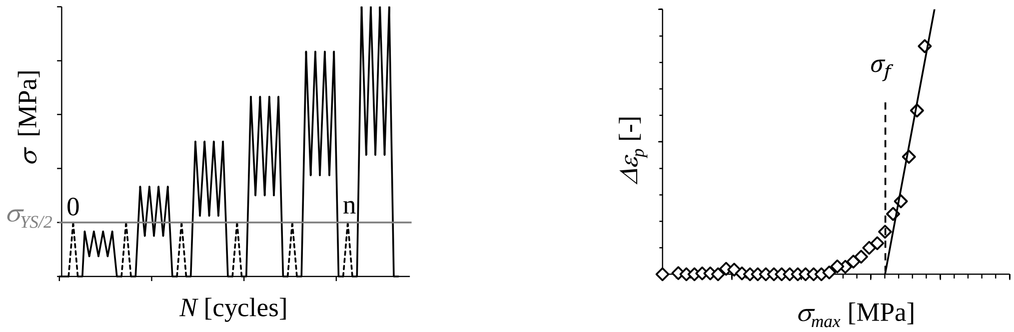

Figure 3. Schematic representation of the stepwise loading test and inelastic strain range versus maximum stress to determine the fatigue limit.

After the fatigue test, the total strain evolution rate ($d\Delta\varepsilon_t/dN$) is analyzed to identify the coalescence of microcracks to a macrocrack. Only the $\Delta\varepsilon_p$ prior to the macrocrack coalescence is used to determine the fatigue damage (D) according to:

$$D = \frac{\Delta\varepsilon_p - \Delta\varepsilon_{p0}}{\Delta\varepsilon_{pf} - \Delta\varepsilon_{p0}} \tag{1}$$

where $\Delta\varepsilon_p$ is the current plastic strain measured for each fatigue block, $\Delta\varepsilon_{p0}$ is the initial inelastic strain, and $\Delta\varepsilon_{pf}$ corresponds to microcrack coalescence inelastic strain.

2.2. Fracture toughness tests

Fracture toughness was evaluated through the Essential Work of Fracture (EWF) methodology based on Elasto-Plastic Fracture Mechanics (EPFM). The method, described in the CWA protocol [8], consists of loading in tension a range of Double Edge Notched Tensile (DENT) specimens with different ligament lengths (l_0). The specimens shown in figure 4 were manufactured by wire erosion and fatigue pre-cracked in a resonance testing machine Rumul Testronic. By testing those specimens up to fracture, it is possible to determine the specific essential work of fracture (w_e) by plotting the specific total work of fracture (w_f) against l_0 as represented in figure 4. The w_f is obtained by integrating the area under the load vs displacement curve for each tested specimen (W_f) and dividing it by the fractured area (l_0t). Equation 2 defines w_e as the intercept and the specific non-essential work of fracture (w_pb) as the slope. Besides separating the w_f the method also allows the separation of the energy required for crack initiation and propagation. The specific work for fracture initiation (w_e^i) is independent of the ligament length. It is determined as the mean value of the specific total work of fracture to crack onset (w_f^i), which is used to define the w_e^i as illustrated in figure 4. The measured w_e and w_e^i are not intrinsic material properties, as they depend on the sheet thickness.

$$\frac{W_f}{l_0 t_0} = w_f = w_e + w_p b l_0 \tag{2}$$

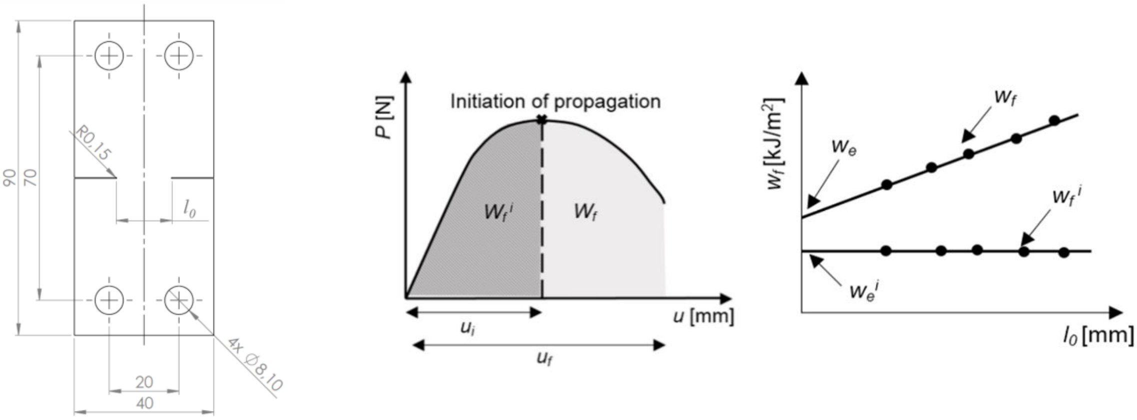

Figure 4. DENT specimen used to determine the EWF (l_0 refers to the different ligament lengths): Schematic representation of the determination of W_f and W_f^i for a given ligament length. Plot of w_f vs l_0, the intercept gives the specific work of fracture, w_e.

At least ten specimens per material were tested in a 250 kN universal testing machine Instron 5585H, equipped with a digital video extensometer. The crosshead testing speed was set at 1 mm/min. The load-displacement measurements were carried out by a video extensometer using initial marks separated by 50 mm. The crack initiation was detected using a high-resolution video camera synchronized with the testing machine. The w_f^i was determined for at least one specimen of each ligament length, and the w_e^i was determined as the mean value.

3. Results and discussion

Figure 5 shows a cross-section of the trimmed specimens for each steel. Sheared edges exhibit the four well-known regions obtained by a shearing process [9]: rollover, smooth or burnish zone, fracture zone and burr (Figure 5). Although the trimming clearance was almost the same, the shape of the trimmed edges was slightly different. The HR CP980 SF presents a longer burnish zone and less rollover than HR CP800 SF and HR DP600.

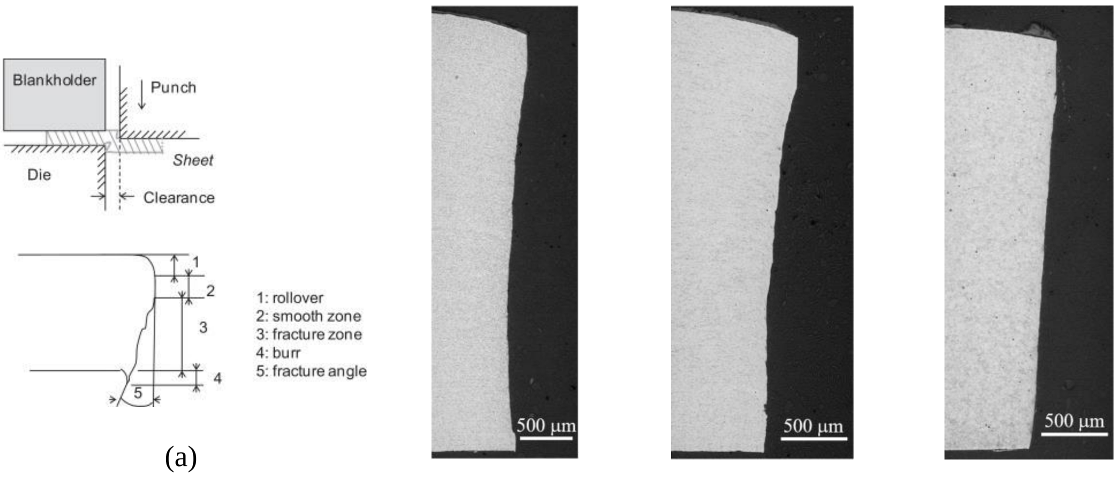

(a) (b) (c) (d)

Figure 5. a) Sheared edge profile characteristics and analysis for: b) HR DP600, c) HR CP800 SF, and d) HR CP980SF.

These differences in the shear edge, related to the material properties, may affect the fatigue resistance as the burr, the defects in the fracture zone or the transition between the burnish to fracture zone act as stress concentration points [4]. Such locally higher stresses induce the nucleation of cracks that propagate throughout the specimen, as observed in figure 6. The fatigue resistance of the polished specimens is driven by the defects or roughness of the as-rolled surface, while the defects in the trimmed edge govern the fatigue behaviour of trimmed specimens. Although the trimmed edge morphology and the resulting defects are similar in all the investigated steels, their effect on the fatigue resistance is different, as observed in the *stiffness test* data shown in figure 7. As expected, the polished conditions can withstand higher stress, i.e. more fatigue blocks, during the rapid fatigue tests than the trimmed specimens.

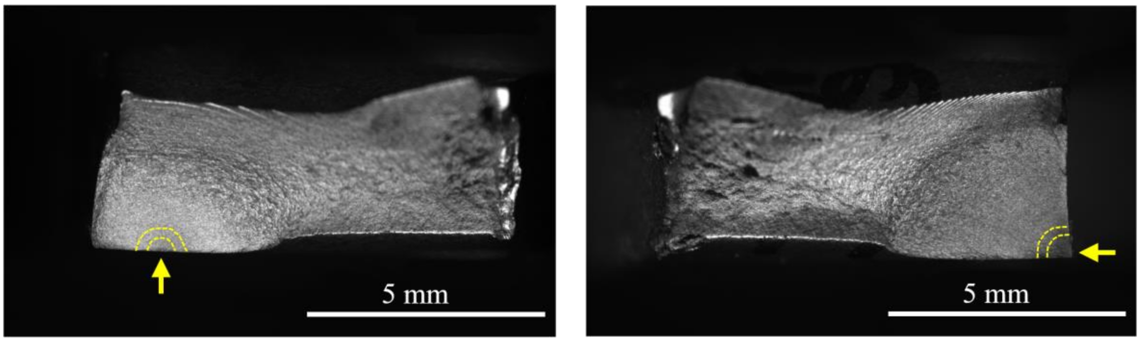

(a) (b)

Figure 6. Fatigue crack initiation and propagation for the HR DP600 in: a) polished, and b) trimmed specimens.

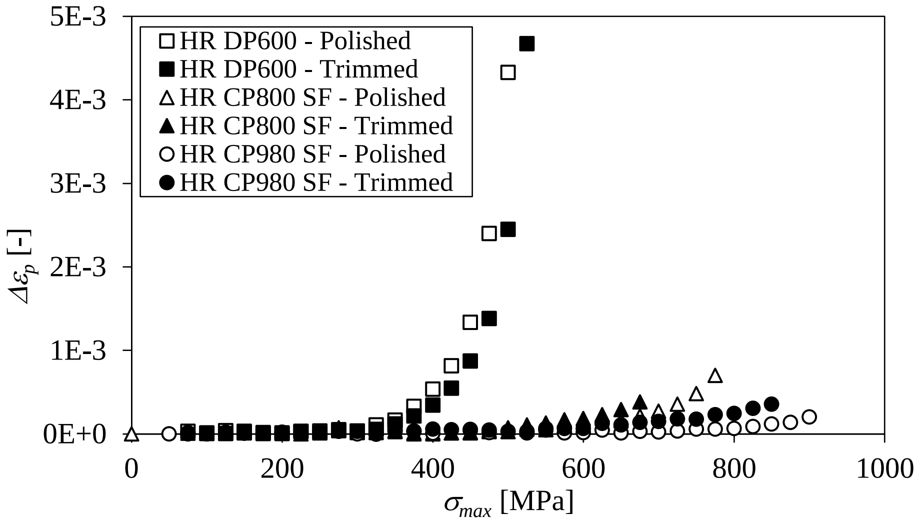

Figure 7. Inelastic strain range versus maximum stress curves from the stiffness method for the polished and trimmed conditions and investigated materials.

As summarized in table 3, the HR CP980 SF exhibits the best fatigue resistance for the polished condition, while the HR DP 600 shows the lowest one. The results obtained by the conventional staircase tests (σ_f) and *stiffness method* ($\sigma_{f\text{-}SM}$) are in good agreement for all the conditions. However, the fatigue resistance of trimmed specimens clearly decreases with respect to the polished conditions in both CP steels compared with the HR DP600. This behaviour is well described by the fatigue strength reduction factor (k_f), and calculated as the ratio between the fatigue resistance of the sheared to polished edges at 10^6 cycles:

$$k_f = \frac{\sigma_{f-Trimmed}}{\sigma_{f-Polished}} \quad (3)$$

Traditionally, it is accepted that σ_f increases by increasing the tensile strength (σ_{UTS}), as shown in figure 8a. However, although it is commonly known that high-strength steels are sensitive to pre-existing defects [10], this relationship does not give enough information for material selection when dealing with high-strength materials and defects. Instead, this information is found in the ability of the material to resist the propagation of damage, as the defects in the trimmed edges in the present work. This behaviour is rationalized by damage tolerance, which is closely linked to fracture toughness, i.e. a tough material better tolerates the pre-existing defects, while a material with a lower toughness is more sensitive to them. Damage tolerance has been conventionally related to σ_{UTS} and ductility, but in high-strength materials, ductility and fracture toughness do not show the same trend [2,11]. In AHSS, fracture toughness, evaluated in the frame of fracture mechanics, better represents the resistance of pre-existent defects. Similarly, fracture toughness expressed in terms of w_e^i (crack propagation resistance at crack initiation) and w_e (overall fracture toughness) can be used to assess the fatigue behaviour of pre-existing defects as it shows a good linear trend with the k_f factor (Figure 8b). Although only material data for the three investigated materials is available the observed trend path the way to further investigations with more materials of different microstructures, strengths, and thicknesses. Materials with low sensitivity to surface defects, i.e. with high damage tolerance, present a k_f close to 1 and have a high w_e value. On the contrary, materials with lower w_e are more sensitive to surface defects, i.e. poor damage tolerance, as the k_f is far below 1. The same trend is observed by plotting the k_f against the w_e^i. Both w_e^i and w_e are good indicators of damage tolerance for AHSS sheets.

Such a good correlation between the fatigue notch sensitivity, in terms of k_f, and the fracture toughness, in terms of w_e and w_e^i, means that the effect of trimming on fatigue can be readily determined by experimentally simple tests, i.e. with a fatigue test in the polished condition and the EWF.

Table 3. Fatigue and fracture toughness results for the three investigated materials: fatigue limit by the conventional tests (σ_f) and from the stiffness method ($\sigma_{f\text{-}SM}$) at R = 0.1 for each edge condition, fatigue strength reduction factor (k_f), fracture toughness (w_e) and fracture toughness at crack initiation (w_e^i).

Steel grade	Edge condition	σ_f [MPa]	$\sigma_{f\text{-}SM}$ [MPa]	k_f	w_e^i [kJ/m^2]	w_e [kJ/m^2]
HR DP600	Polished	502 ± 5	465 ± 10	0.98	285 ± 29	481 ± 67
	Trimmed, Cl = 7%	470 ± 5	454 ± 20			
HR CP800 SF	Polished	622 ± 9	619 ± 16	0.73	155 ± 28	299 ± 56
	Trimmed, Cl = 8.8%	426 ± 19	449 ± 11			
HR CP980 SF	Polished	643 ± 30	678 ± 14	0.68	107 ± 18	141 ± 45
	Trimmed, Cl = 8.6%	429 ± 11	464 ± 67			

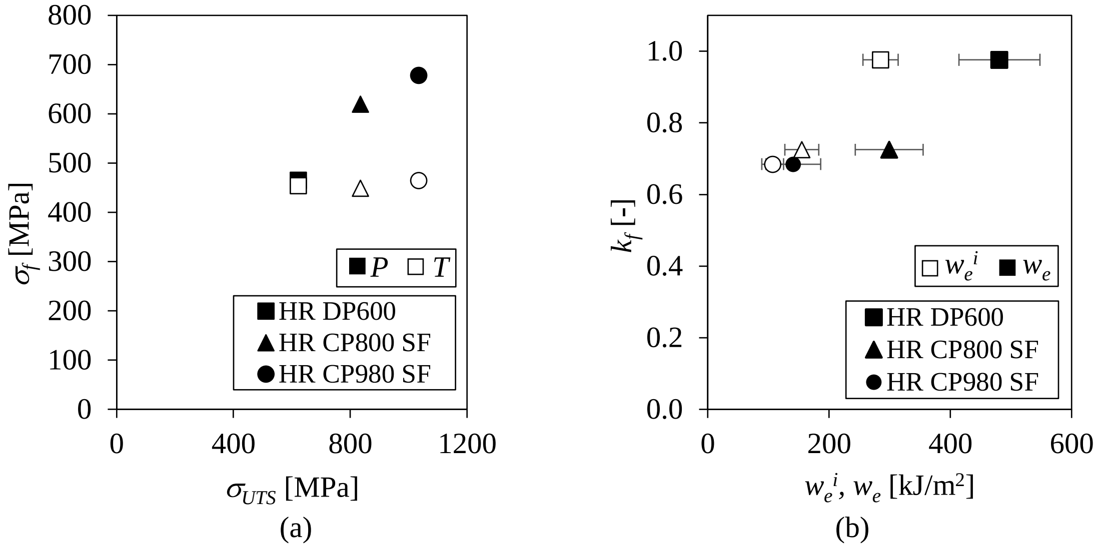

Figure 8. a) Fatigue resistance of polished (P) and trimmed (T) specimens against tensile strength (σ_{UTS}) for the investigated AHSS between 3 to 4mm. b) Fatigue strength reduction factor (k_f) as a function of specific work for fracture initiation (w_e^i) and specific essential work of fracture (w_e).

4. Summary and conclusions

The results obtained in this work show that fracture toughness can be used to assess the fatigue strength reduction of AHSS. The following conclusions can be drawn:

- The fatigue resistance can be readily determined through the stiffness method, in a quick and reliable way, for both polished and sheared specimens.
- The fatigue strength reduction due to the sheared edge can be expressed as a fatigue strength reduction factor, k_f, which shows an excellent correlation to the fracture toughness measured in terms of the EWF. It means that tougher materials have lower fatigue notch sensitivity.
- The proposed approach allows to rapidly determine the influence of the trimmed edge on the fatigue resistance of AHSS through a rapid test in the polished conditions and the fracture toughness obtained with the EWF method.

Acknowledgements

The research leading to these results has received funding from the European Union's Horizon 2020 innovation action programme under grant agreement No 101006844 – Fatigue4Light project. This work was financially supported by the Catalan Government through the funding grant ACCIÓ-Eurecat (Project PRIV - RapidFat). A.M. acknowledges the Agència de Gestió d'Ajuts Universitaris i de Recerca (AGAUR) del Departament de Recerca i Universitats de la Generalitat de Catalunya for recognising the Microstructural Design and Advanced Manufacturing of Materials Group as a consolidated research group number 2021 SGR 01053.

References

[1] Han S, Chang Y, Wang C Y and Dong H 2022 *J. Mater. Process. Technol.* **299** 117377
[2] Frómeta D, Lara A, Grifé L, Dieudonné T, Dietsch P, Rehrl J, Suppan C, Casellas D and Calvo J 2021 *Metall. Mater. Trans. A Phys. Metall. Mater. Sci.* **52** 840–56
[3] Gläsner T, Sunderkötter C, Plath A, Bednarz M, Volk W, Hoffmann H and Golle R 2014 *Key Eng. Mater.* **611–612** 1294–307
[4] Stahl J, Pätzold I, Golle R, Sunderkötter C, Sieurin H and Volk W 2020 *J. Manuf. Mater. Process. 2020, Vol. 4, Page 52* **4** 52
[5] Parareda S, Lara A, Sieurin H, Darmas H and Casellas D 2018 *MATEC Web Conf.* **165** 1–6

[6] Dixon W J and Mood A M 1948 *J. Am. Stat. Assoc.* **43** 109–26
[7] Parareda S, Casellas D, Lara A and Mateo A 2022 *Int. J. Fatigue* **156** 106643
[8] EUROPEAN COMMITTEE FOR STANDARDIZATION 2021 *Test method for determination of the essential work of fracture of thin ductile metallic sheets* (Brussels: CEN)
[9] The Association of German Engineers 1994 *VDI 2906-2: Quality of cut faces of (sheet) metal parts after cutting, blanking, trimming or piercing; general introduction, characteristic values, materials* (Berlin: Beuth)
[10] Lara A, Picas I and Casellas D 2013 *J. Mater. Process. Technol.* **213** 1908–19
[11] Frómeta D, Parareda S, Lara A, Molas S, Casellas D, Jonsén P and Calvo J 2020 *Eng. Fract. Mech.* **229** 106949